Int. J. Solids Structures, Vol. 17, No. 12, pp. 1179–1202, 1981
Printed in Great Britain.

0020-7683/81/121179-24$02.00/0
Pergamon Press Ltd.

A TWO-DIMENSIONAL THEORY FOR PIEZOELECTRIC LAYERS USED IN ELECTRO-MECHANICAL TRANSDUCERS—II

APPLICATIONS

N. BUGDAYCI and D. B. BOGY
Department of Mechanical Engineering, University of California, Berkeley, CA 94720, U.S.A.

(*Received* 5 *December* 1980)

Abstract—The approximate 2-D theory derived in Part I is applied here to the time harmonic problems of plane-strain and axisymmetry. Also, the transient axisymmetric solution is obtained for a circular layer that is suddenly released from a transverse concentrated central load on one face and an opposing ring load along the outer edge of the other face. For this problem the output voltage is computed as a function of time when the crystal is an element in a known electrical circuit.

1. INTRODUCTION

This paper is a continuation of Part I, which appears as the preceeding article in this same journal issue and is designated as Ref. [1]. Many of the equations in [1] will be required for the analysis presented here, and they will be referenced with the assumption that the reader has access to that paper.

In [1] an Nth order approximate 2-D theory was developed for strongly coupled piezoelectric ceramic layers that are used in electro-mechanical transducers. It was found that the first order theory was the lowest that yields an electro-mechanical coupling. The dispersion curves were obtained for harmonic waves in the layer for both the 3-D and the first and second order approximate 2-D theories.

In this Part II, we present general Nth order theory solutions for steady state time-harmonic motions of plane-strain and axisymmetry. We also obtain the transient axisymmetric solution for a circular layer that is supported along its outer edge, loaded transversely at its center, and then released from this loading so that transient free vibrations occur. The layer with electroded faces is assumed to be an element in a circuit with known electrical impedance, and the voltage between the layer electrodes is derived as a function of time.

In Section 2 the general circuit equation is derived, and it is found that the output voltage is associated only with the extensional modes of motion. The steady state time-harmonic plane-strain solution is derived in Section 3. The time-harmonic axisymmetric problem is treated in Section 4, and the transient axisymmetric case is solved in Section 5. Section 6 contains the numerical results of this solution for a particular loading and crystal. A brief discussion is given in Section 7.

2. DERIVATION OF CIRCUIT EQUATION

In this section we consider layers with cylindrical edge boundaries as shown in Fig. 1 of [1] for two shapes of the boundary curve C. In each problem the faces of the layer are electroplated and therefore are equipotential surfaces. The edges are directly in contact with a non-conducting medium, so the currents across them vanish.

When such a layer is the active element of a circuit, the voltage difference is determined by the current equation

$$I = YV \tag{2.1}$$

where V, Y and I stand for the voltage difference, the circuit admittance and the current, respectively. In order to make use of this equation we need an expression for the current in terms of the 2-D field variables of the approximate theory. The current across a surface S is

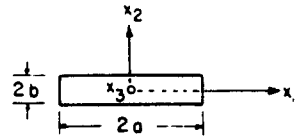

Fig. 1. Layer cross section for the case of plane strain.

given by

$$I = \frac{\mathrm{d}}{\mathrm{d}t}\int_S D_i n_i \,\mathrm{d}S. \tag{2.2}$$

Integrating the 3-D electric displacement field equation (2.2) of [1] over the volume of the layer, applying the divergence theorem, differentiating with respect to time, and, finally, recalling (2.2), we obtain the result that the total current across the boundaries of the layer is equal to zero. Since we have already assumed that the current across the edge boundary vanishes, this implies

$$\frac{\mathrm{d}}{\mathrm{d}t}\int_A D_2^+ \,\mathrm{d}A - \frac{\mathrm{d}}{\mathrm{d}t}\int_A D_2^- \,\mathrm{d}A = 0 \tag{2.3}$$

where A is the area of the middle plane of the layer and D^+ and D^- denote D evaluated at $x_2 = b$ and $x_2 = -b$, respectively. Designating by D_{2o} and D_{2e} the odd and even components of D_2 with respect to the x_2-coordinate, we can rewrite (2.3) as

$$\frac{\mathrm{d}}{\mathrm{d}t}\int_A D_{2o}^+ \,\mathrm{d}A = 0. \tag{2.4}$$

The current that enters the layer through the lower face is then equal to the current that leaves it through the upper face and is given by

$$I = \frac{\mathrm{d}}{\mathrm{d}t}\int_A D_{2e}^+ \,\mathrm{d}A. \tag{2.5}$$

By application of the divergence theorem to the upper half of the layer only, this is found to be equal also to the current across the middle plane

$$I = \frac{\mathrm{d}}{\mathrm{d}t}\int_A D_2^0 \,\mathrm{d}A = \frac{\mathrm{d}}{\mathrm{d}t}\int_A D_{2e}^0 \,\mathrm{d}A \tag{2.6}$$

where D_2^0 denotes D_2 evaluated at $x_2 = 0$.

The 3-D constitutive equation for D_{2e} involves only extensional variables

$$D_{2e} = e_{21}(u_{1e,1} + u_{3e,3}) + e_{22}u_{2o,2} - \epsilon_{22}\phi_{o,2} \tag{2.7}$$

where subscripts "e" and "o" denote the even and odd parts of the functions with respect to $x_2 = 0$. The series expansions for these variables are

$$u_{\gamma e} = \sum_{k=0}^{R} u_\gamma^{(2k)} \cos k\pi(1-\psi), \qquad u_{2o} = \sum_{k=0}^{S} u_2^{(2k+1)} \cos\frac{(2k+1)\pi}{2}(1-\psi),$$

$$\phi_o = B(t)\psi + \sum_{k=1}^{R} \phi^{(2k)} \sin k\pi(1-\psi) \tag{2.8}$$

where integers R and S were defined in (4.5) of [1] for the Nth order approximate theory. We

substitute (2.8) into (2.7) and obtain for $x_2 = 0$,

$$D_{2e}^0 = -\epsilon_{22}\frac{B(t)}{b} + \sum_{k=0}^{R}\left\{(-1)^k\left[e_{21}u_{\gamma,\gamma}^{(2k)} + \epsilon_{22}\left(\frac{k\pi}{b}\right)\phi^{(2k)}\right]\right\} + e_{22}\sum_{k=0}^{S}\left\{(-1)^k\frac{(2k+1)\pi}{2b}u_2^{(2k+1)}\right\}. \tag{2.9}$$

Then using (2.6) we find

$$I = -A\epsilon_{22}\frac{\dot{B}(t)}{b} + \sum_{k=0}^{R}\left\{(-1)^k\int_A\left[e_{21}\dot{u}_{\gamma,\gamma}^{(2k)} + \frac{k\pi}{b}\epsilon_{22}\dot{\phi}^{(2k)}\right]dA\right\} + e_{22}\sum_{k=0}^{S}\left\{(-1)^k\frac{(2k+1)\pi}{2b}\int_A\dot{u}_2^{(2k+1)}\,dA\right\}. \tag{2.10}$$

Now, substitution of

$$B(t) = \frac{1}{2}V(t) \tag{2.11}$$

along with (2.10) into (2.1) yields the circuit equation in terms of the two-dimensional field variables

$$\sum_{k=0}^{R}\left\{(-1)^k\int_A\left[e_{21}\dot{u}_{\gamma,\gamma}^{(2k)} + \epsilon_{22}\frac{k\pi}{b}\dot{\phi}^{(2k)}\right]dA\right\} + e_{22}\sum_{k=0}^{S}\left\{(-1)^k\frac{(2k+1)\pi}{2b}\int_A\dot{u}_2^{(2k+1)}\,dA\right\} = \left(YV + \frac{A\epsilon_{22}}{2b}\dot{V}\right). \tag{2.12}$$

An important result from the point of view of transducer applications can be discerned by inspection of field equations (3.33) of [1] and, when the layer is the active element of a circuit, also the circuit equation (2.12). For a passive layer with faces constrained to be equipotential surfaces, the imposed voltage difference between the two faces effects only extensional variables; and only the extensional variables determine the voltage difference when the layer is the active element. That is, the voltage difference, for the type of crystal considered here, does not alter and is insensitive to the flexural modes of motion. This can also be deduced from the relevant three-dimensional equations.

3. STEADY-STATE PLANE STRAIN MOTION IN A RECTANGULAR LAYER

The layer considered in this problem and the coordinate system used in the study of its motion are shown in Fig. 1. Its length is infinite along the x_3-axis, it has thickness $2b$ along the x_2-axis and width $2a$ along the x_1-axis.

We examine steady-state plain strain motion and account for the time-dependence of the field variables through a harmonic term $e^{i\omega t}$, where ω is the frequency. Thus, if a function g represents a time-dependent field variable, we define the corresponding complex valued time-independent variable $\bar{g}$ by

$$g(x_1, x_2, x_3, t) = \mathrm{Re}\{\bar{g}(x_1, x_2, x_3)\,e^{i\omega t}\}.$$

For convenience we will delete the superposed bar and use the same notation for the two functions. For plane strain u_3 and $u_3^{(n)}$ vanish throughout the plate and all functions are independent of x_3. Therefore, the variables T_{ij}, D_i, u_i and ϕ depend on x_1 and x_2 and the variables $T_{ij}^{(n)}$, $D_i^{(n)}$, $u_i^{(n)}$ and $\phi^{(n)}$ depend on x_1 only.

The boundary conditions at the faces and the edges of the layer are specified by

$$\begin{aligned} T_{21}(x_1, b) &= T_{21}^{+}(x_1); \qquad T_{21}(x_1, -b) = T_{21}^{-}(x_1) \\ T_{22}(x_1, b) &= T_{22}^{+}(x_1); \qquad T_{22}(x_1, -b) = T_{22}^{-}(x_1) \\ T_{23}(x_1, \pm b) &= 0 \\ \phi(x_1, b) &= \phi^{+} = \text{const.} \\ \phi(x_1, -b) &= \phi^{-} = \text{const.} \end{aligned} \tag{3.1}$$

$$\begin{aligned} T_{11}(a, x_2) &= \bar{T}_{11}^{+}(x_2); \qquad T_{11}(-a, x_2) = \bar{T}_{11}^{-}(x_2) \\ T_{12}(a, x_2) &= \bar{T}_{12}^{+}(x_2); \qquad T_{12}(-a, x_2) = \bar{T}_{12}^{-}(x_2) \\ T_{13}(\pm a, x_2) &= 0; \qquad D_1(\pm a, x_2) = 0. \end{aligned} \tag{3.2}$$

Specifying the appropriate displacement components at the edges instead of the stress components indicated in (3.2) would also be acceptable.

We note here that the solution of the problem stated above for the infinite rectangular layer is identical to the solution of the similar problem for a finite rectangular layer with the following additional boundary conditions at the ends, $x_3 = \pm c$.

$$u_3 = 0; \quad T_{31} = T_{32} = 0; \quad D_3 = 0 \quad \text{at} \quad x_3 = \pm c. \tag{3.3}$$

This can be verified by considering the constitutive equations (2.3) and (2.4) of [1] for plane strain conditions and observing that the boundary conditions (3.3) at the ends are satisfied at any perpendicular cross section of the layer.

For steady-state plain strain motion of a layer with equipotential faces, the 2-D field equations (3.33) of [1] reduce to the following:

$$\begin{aligned} &(1+\delta_{no})c_{11}u_{1,11}^{(n)} + \frac{\pi}{2b}\sum_{m=0}^{N}\{D_{mn}u_{2,1}^{(m)}\} \\ &-\frac{n\pi}{2b}(e_{21}+e_{16})\phi_{,1}^{(n)} + \left[\rho\omega^2(1+\delta_{no}) - \left(\frac{n\pi}{2b}\right)^2 c_{44}\right]u_1^{(n)} \\ &= -\frac{1}{b}F_1^{(n)} \quad \text{for} \quad n = 0, 1, \ldots, N \\ &(1+\delta_{no})c_{44}u_{2,11}^{(n)} + \sum_{m=1}^{N}\{B_{mn}e_{16}\phi_{,11}^{(m)}\} \\ &-\frac{\pi}{2b}\sum_{m=0}^{N}\{D_{nm}u_{1,1}^{(m)}\} + \left[\rho\omega^2(1+\delta_{no}) - \left(\frac{n\pi}{2b}\right)^2 c_{22}\right]u_2^{(n)} \\ &+\left(\frac{\pi}{2b}\right)^2\sum_{m=1}^{N}\{B_{nm}mne_{22}\phi^{(m)}\} = \frac{-1}{b}F_2^{(n)} + \frac{n\pi}{2b}B_{no}\frac{1}{b}e_{22}B \quad \text{for} \quad n = 0, 1, \ldots, N \\ &\sum_{m=0}^{N}\{B_{nm}e_{16}u_{2,11}^{(m)}\} - \epsilon_{11}\phi_{,11}^{(n)} + \frac{n\pi}{2b}(e_{16}+e_{21})u_{1,1}^{(n)} \\ &+\left(\frac{\pi}{2b}\right)^2\sum_{m=0}^{N}\{B_{mn}mne_{22}u_2^{(m)}\} + \left(\frac{n\pi}{2b}\right)^2\epsilon_{22}\phi^{(n)} = 0 \quad \text{for} \quad n = 1, 2, \ldots, N. \end{aligned} \tag{3.4}$$

We solve the set of coupled second order ordinary differential equations (3.4) by first transforming it into a set of first order ordinary differential equations. For this purpose we

define $3N+2$ functions $z_j^{(n)}(x_1)$ as follows:

$$z_1^{(n)} = (1+\delta_{no})c_{11}u_{1,1}^{(n)} + \frac{\pi}{2b}\sum_{m=0}^{N}\{D_{mn}u_2^{(m)}\} - \frac{n\pi}{2b}(e_{21}+e_{16})\phi^{(n)} \quad n=0,1,\ldots,N$$

$$z_2^{(n)} = (1+\delta_{no})c_{44}u_{2,1}^{(n)} + \sum_{m=1}^{N}\{B_{mn}e_{16}\phi_{,1}^{(m)}\} - \frac{\pi}{2b}\sum_{m=0}^{N}\{D_{nm}u_1^{(m)}\} \quad n=0,1,\ldots,N$$

$$z_3^{(n)} = \sum_{m=0}^{N}\{B_{nm}e_{16}u_{2,1}^{(m)}\} - \epsilon_{11}\phi_{,1}^{(n)} + \frac{n\pi}{2b}(e_{16}+e_{21})u_1^{(n)} \quad n=1,2,\ldots,N. \tag{3.5}$$

With these definitions, we can rewrite (3.4) in the following form:

$$z_{1,1}^{(n)} = \left[\left(\frac{n\pi}{2b}\right)^2 c_{44} - \rho\omega^2(1+\delta_{no})\right]u_1^{(n)} - \frac{1}{b}F_1^{(n)} \quad n=0,1,\ldots,N$$

$$z_{2,1}^{(n)} = \left[\left(\frac{n\pi}{2b}\right)^2 c_{22} - \rho\omega^2(1+\delta_{no})\right]u_2^{(n)} - \left(\frac{\pi}{2b}\right)^2\sum_{m=1}^{N}\{B_{nm}mne_{22}\phi^{(m)}\} - \frac{1}{b}F_2^{(n)}$$
$$+\frac{n\pi}{2b}B_{no}\frac{1}{b}e_{22}B \quad n=0,1,\ldots,N$$

$$z_{3,1}^{(n)} = -\left(\frac{\pi}{2b}\right)^2\sum_{m=0}^{N}\{B_{mn}mne_{22}u_2^{(m)}\} - \left(\frac{n\pi}{2b}\right)^2\epsilon_{22}\phi^{(n)} \quad n=1,2,\ldots,N. \tag{3.6}$$

Now, $3N+2$ linear equations (3.5) can be solved for $3N+2$ functions $u_{1,1}^{(n)}$, $u_{2,1}^{(n)}$ ($n=0,1,\ldots,N$) and $\phi_{,1}^{(n)}$ ($n=1,2,\ldots,N$). The solutions will be linear combinations of functions $u_1^{(n)}$, $u_2^{(n)}$, $z_1^{(n)}$, $z_2^{(n)}$ ($n=0,1,\ldots,N$) and $\phi^{(n)}$, $z_3^{(n)}$ ($n=1,2,\ldots,N$). Combining these solutions with (3.6), we can then construct a set of first order ordinary differential equations expressible in the following matrix form.

$$\underset{\sim}{y}_{,1} = \underset{\sim}{A}\underset{\sim}{y} + \underset{\sim}{d}. \tag{3.7}$$

In (3.7) $\underset{\sim}{y}(x_1)$ is the $(6N+4)\times 1$ array of the unknown functions, and it is given in transposed form by

$$\underset{\sim}{y}^T(x_1) = \{y_1(x_1),\ldots,y_{6N+4}(x_1)\} = \{u_1^{(0)}(x_1),\ldots,u_1^{N}(x_1),u_2^{(0)}(x_1),\ldots,u_2^{(N)}(x_1),$$
$$\phi^{(1)}(x_1),\ldots,\phi^{(N)}(x_1),z_1^{(0)}(x_1),\ldots,z_1^{(N)}(x_1),$$
$$z_2^{(0)}(x_1),\ldots,z_2^{(N)}(x_1),z_3^{(1)}(x_1),\ldots,z_3^{(N)}(x_1)\}. \tag{3.8}$$

$\underset{\sim}{A}$ is a $(6N+4)\times(6N+4)$ matrix. Its elements depend on the material constants and the frequency only. $\underset{\sim}{d}(x_1)$ is the $(6N+4)\times 1$ array of forcing functions. Its non-zero elements are the non-homogeneous terms on the right hand sides of eqns (3.6).

The complete general solution to a set of coupled first order ordinary differential equations of the type (3.7) is given, e.g. in Chap. 5 of Ref. [2]. For (3.7), in particular, the solution is:

$$\underset{\sim}{y}(x_1) = \underset{\sim}{W}(x_1)\underset{\sim}{c} + \underset{\sim}{W}(x_1)\int_{-a}^{x_1}\underset{\sim}{W}^{-1}(x)\underset{\sim}{d}(x)\,dx. \tag{3.9}$$

In (3.9) $\underset{\sim}{c}$ is an $(6N+4)\times 1$ array of arbitrary constants while $\underset{\sim}{W}(x_1)$ is a $(6N+4)\times(6N+4)$ matrix called the standard fundamental matrix of the homogeneous system and it is given by

$$\underset{\sim}{W}(x_1) = \underset{\sim}{P}\underset{\sim}{V}(x_1) \tag{3.10}$$

where $\underset{\sim}{V}(x_1)$ is the diagonal matrix with the diagonal elements,

$$V_{rr}(x_1) = e^{\lambda_r x_1} \quad \text{(no summation on } r) \tag{3.11}$$

The λ_1 to $\lambda_{(6N+4)}$ are the eigenvalues of $\underset{\sim}{A}$. $\underset{\sim}{P}$ is the matrix whose rth column is an eigenvector of $\underset{\sim}{A}$ corresponding to λ_r.

The elements of the arbitrary array $\underset{\sim}{c}$ are determined by the edge boundary conditions. For traction-free edges across which no current flows, the boundary conditions are:

$$\begin{aligned} &T_{11}^{(n)}(x_1) = 0 \quad \text{at} \quad x_1 = \pm a \quad \text{for} \quad n = 0, \ldots, N \\ &T_{12}^{(n)}(x_1) = 0 \quad \text{at} \quad x_1 = \pm a \quad \text{for} \quad n = 0, \ldots, N \\ &\tilde{D}_1^{(n)}(x_1) = 0 \quad \text{at} \quad x_1 = \pm a \quad \text{for} \quad n = 1, \ldots, N. \end{aligned} \tag{3.12}$$

By means of the appropriate field equations we can express the boundary conditions (3.12) in terms of the values of the two-dimensional variables $u_j^{(n)}$ and $\phi^{(n)}$ at $x_1 = \pm a$. Substituting next the solution from (3.9), we would obtain $(6N+4)$ linear equations in the $(6N+4)$ unknown elements of $\underset{\sim}{c}$ which we could then solve to completely determine the solution.

When the layer is the active element of a circuit, B is an additional unknown. The additional equation associated with it is derived by substituting the solution (3.9) into the circuit equation (2.12) and carrying out the indicated integrations over the middle surface area of a unit-length section of the layer. The values for A and Y to be used in that equation are those corresponding to such a section of unit length.

The preceding is an outline of a method of obtaining the exact solution for the present problem using the field equations deduced from an approximate theory of arbitrarily large order N. In the actual solution of the problem the calculations can be much simplified by handling the extensional and flexural variables separately, as these always uncouple. It may also be worthwhile in this case to separate the component of the motion that is symmetric with respect to the x_1-coordinate from that which is anti-symmetric. This is possible not only becuase of the structure of the field equations which allows such a separation but also because of the symmetry of the edge boundaries with respect to the $x_2 - x_3$ plane.

4. STEADY-STATE AXISYMMETRIC MOTION OF A CIRCULAR LAYER

The layer we consider in this section has thickness $2b$ and radius a. The polar cylindrical coordinate system is shown in Fig. 2. Restricting the study to axisymmetric motions, we require all functions to be independent of the θ-coordinate. In this case the constitutive equations (2.3) of [1] become

$$\begin{aligned} T_{rr} &= c_{11}u_{r,r} + c_{13}\frac{1}{r}u_r + c_{12}u_{z,z} + e_{21}\phi_{,z} \\ T_{\theta\theta} &= c_{13}u_{r,r} + c_{11}\frac{1}{r}u_r + c_{12}u_{z,z} + e_{21}\phi_{,z} \\ T_{rz} &= c_{44}(u_{r,z} + u_{z,r}) + e_{16}\phi_{,r} \\ T_{zz} &= c_{12}\frac{1}{r}(ru_r)_{,r} + c_{22}u_{z,z} + e_{22}\phi_{,z} \\ D_r &= e_{16}(u_{r,z} + u_{z,r}) - \epsilon_{11}\phi_{,r} \\ D_z &= e_{21}\frac{1}{r}(ru_r)_{,r} + e_{22}u_{z,z} - \epsilon_{22}\phi_{,z} \\ T_{r\theta} &= T_{z\theta} = 0; \quad D_\theta = 0. \end{aligned} \tag{4.1}$$

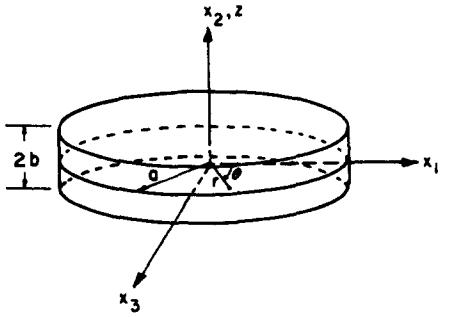

Fig. 2. Geometry and coordinate system for the circular layer.

The 2-D polar mechanical displacement, electric potential, stress and electric displacement components are determined from the following equations for the Nth order approximate theory.

$$u_r(r, z, t) = \sum_{n=0}^{N} u_r^{(n)}(r, t) \cos\frac{n\pi}{2}(1-\psi)$$

$$u_z(r, z, t) = \sum_{n=0}^{N} u_z^{(n)}(r, t) \cos\frac{n\pi}{2}(1-\psi)$$

$$\phi(r, z, t) = A + B\psi + \sum_{n=1}^{N} \phi^{(n)}(r, t) \sin\frac{n\pi}{2}(1-\psi)$$

$$(T_{rr}^{(n)}, T_{\theta\theta}^{(n)}, T_{zz}^{(n)}, T_{rz}^{(n)}) = \int_{-1}^{1} (T_{rr}, T_{\theta\theta}, T_{zz}, T_{rz}) \cos\frac{n\pi}{2}(1-\psi)\,d\psi$$

$$(\bar{T}_{rr}^{(n)}, \bar{T}_{\theta\theta}^{(n)}, \bar{T}_{zz}^{(n)}, \bar{T}_{rz}^{(n)}) = \int_{-1}^{1} (T_{rr}, T_{\theta\theta}, T_{zz}, T_{rz}) \sin\frac{n\pi}{2}(1-\psi)\,d\psi$$

$$(D_r^{(n)}, D_z^{(n)}) = \int_{-1}^{1} (D_r, D_z) \cos\frac{n\pi}{2}(1-\psi)\,d\psi$$

$$(\bar{D}_r^{(n)}, \bar{D}_z^{(n)}) = \int_{-1}^{1} (D_r, D_z) \sin\frac{n\pi}{2}(1-\psi)\,d\psi$$

$$u_\theta^{(n)} = 0; \quad T_{\theta r}^{(n)} = T_{\theta z}^{(n)} = \bar{T}_{\theta r}^{(n)} = \bar{T}_{\theta r}^{(n)} = 0; \quad D_\theta^{(n)} = \bar{D}_\theta^{(n)} = 0. \tag{4.2}$$

From (4.1) and (4.2) we derive only the 2-D constitutive equations that will be needed

$$T_{rr}^{(n)} = (1+\delta_{no})c_{11}u_{r,r}^{(n)} + (1+\delta_{no})c_{13}\frac{1}{r}u_r^{(n)} + \frac{\pi}{2b}c_{12}\sum_{m=1}^{N}\{mB_{mn}u_z^{(m)}\}$$

$$-\frac{\pi}{2b}e_{21}n\phi^{(n)} + 2\delta_{no}e_{21}\frac{B}{b}$$

$$T_{rz}^{(n)} = (1+\delta_{no})c_{44}u_{z,r}^{(n)} + e_{16}\sum_{m=1}^{N}\{B_{mn}\phi_{,r}^{(m)}\} + \frac{\pi}{2b}c_{44}\sum_{m=1}^{N}\{mB_{mn}u_r^{(m)}\}$$

$$\bar{D}_r^{(n)} = e_{16}\sum_{m=0}^{N}\{B_{nm}u_{z,r}^{(m)}\} - \epsilon_{11}\phi_{,r}^{(n)} + \frac{\pi}{2b}e_{16}nu_r^{(n)}. \tag{4.3}$$

At this point we impose the further restriction of time-harmonic motion, and, as in the previous section, change to time-independent variables without change in notation. The conversion of 2-D Cartesian displacement components into the 2-D polar displacement components follows the same rules as in the 3-D analysis. On this basis, the displacement-electric potential equations of motion (3.33) of [1] can be directly transformed into the following

equations in polar coordinates

$$(1+\delta_{no})c_{11}\mathscr{B}_1(u_r^{(n)})-\frac{n\pi}{2b}(e_{21}+e_{16})\phi_{,r}^{(n)}+\sum_{m=0}^{N}\left\{\frac{\pi}{2b}D_{mn}u_{z,r}^{(m)}\right\}$$

$$+\left[(1+\delta_{no})\rho\omega^2-\left(\frac{n\pi}{2b}\right)^2 c_{44}\right]u_r^{(n)}=\frac{-1}{b}F_r^{(n)}\quad\text{for}\quad n=0,1,\ldots,N$$

$$(1+\delta_{no})c_{44}\mathscr{B}_0(u_z^{(n)})+\sum_{m=1}^{N}\{e_{16}B_{mn}\mathscr{B}_0(\phi^{(m)})\}-\frac{\pi}{2b}\sum_{m=0}^{N}\{D_{nm}\frac{1}{r}(ru_r^{(m)})_{,r}\}$$

$$+\left[(1+\delta_{no})\rho\omega^2-\left(\frac{n\pi}{2b}\right)^2 c_{22}\right]u_z^{(n)}+\left(\frac{\pi}{2b}\right)^2 e_{22}\sum_{m=0}^{N}\{B_{nm}mn\phi^{(m)}\}$$

$$=\left(\frac{n\pi}{2b}\right)B_{no}e_{22}\frac{B}{b}-\frac{1}{b}F_z^{(n)}\quad\text{for}\quad n=0,1,\ldots,N$$

$$e_{16}\sum_{m=0}^{N}\{B_{nm}\mathscr{B}_0(u_z^{(m)})\}-\epsilon_{11}\mathscr{B}_0(\phi^{(n)})+\left(\frac{n\pi}{2b}\right)(e_{16}+e_{21})\frac{1}{r}(ru_r^{(n)})_{,r}$$

$$+\left(\frac{\pi}{2b}\right)^2 e_{22}\sum_{m=1}^{N}\{B_{mn}mnu_z^{(m)}\}+\left(\frac{n\pi}{2b}\right)^2\epsilon_{22}\phi^{(n)}=0\quad\text{for}\quad n=1,2,\ldots,N. \tag{4.4}$$

In (4.4) $\mathscr{B}_k$ is the Bessel differential operator defined by,

$$\mathscr{B}_k=\left(\frac{d^2}{dr^2}+\frac{1}{r}\frac{d}{dr}-\frac{k^2}{r^2}\right),\qquad k=0,1 \tag{4.5}$$

and $F_r^{(n)}$ and $F_z^{(n)}$ are determined by,

$$F_r^{(n)}=\frac{F_1^{(n)}}{\cos\theta}=\frac{F_3^{(n)}}{\sin\theta};\qquad F_z^{(n)}=F_2^{(n)}. \tag{4.6}$$

We now solve these equations by the use of finite Hankel transforms. For this purpose we define values $\lambda_1,\lambda_2,\ldots$ as the positive roots of the equation,

$$J_1(\lambda_p a)=0 \tag{4.7}$$

where J_k denotes the Bessel function of the first kind of order k. By the theory of Bessel functions λ_p are also the roots of

$$\frac{d}{dr}J_0(\lambda_p r)\Big|_{r=a}=0 \tag{4.8}$$

or simply,

$$J_0'(\lambda_p a)=0. \tag{4.9}$$

We note here that $\lambda_0=0$ is also a solution of (4.7) and (4.9).

We denote the finite Hankel transform of order k of a function $g(r)$ evaluated at λ_p by

$$\mathscr{H}_k[g;r\to\lambda_p]=\bar{g}_k(\lambda_p)=\int_0^a rg(r)J_k(\lambda_p r)\,dr. \tag{4.10}$$

The inversion formula for $k=1$ is (see [3], p. 83).

$$g(r)=\frac{2}{a^2}\sum_{\lambda_p>0}\bar{g}_1(\lambda_p)\frac{J_1(\lambda_p r)}{[J_0(\lambda_p a)]^2}, \tag{4.11}$$

while the inversion formula for $k = 0$ is (see [4], p. 597).

$$g(r) = \frac{2}{a^2} \sum_{\lambda_p \geq 0} \bar{g}_0(\lambda_p) \frac{J_0(\lambda_p r)}{[J_0(\lambda_p a)]^2}. \tag{4.12}$$

The inversion formula (4.12) is valid in the closed interval $[0, a]$. However, the inversion formula (4.11) is valid only in the open interval $(0, a)$ and it always produces the zero value at the end points of the interval. Therefore before taking the finite first order Hankel transform of a function, we decompose it into two functions, one that vanishes at the boundaries and another that yields the boundary values. For example, the function $u_r^{(n)}(r)$, which for axisymmetric motion vanishes at $r = 0$, can be decomposed in the following way.

$$u_r^{(n)}(r) = f^{(n)}(r) + C^{(n)} r \tag{4.13}$$

where

$$f^{(n)}(0) = f^{(n)}(a) = 0; \qquad C^{(n)} = a^{-1} u_r^{(n)}(a). \tag{4.14}$$

After substituting (4.13) into (4.4), we apply the first order finite Hankel transform to the first of (4.4) and the zero order finite Hankel transform to the second and third of (4.4). This will be done separately for positive values of λ_p and for λ_0. The following notation will be used to denote first and zero order finite Hankel transforms of a function $g(r)$.

$$\begin{aligned} \bar{g}(\lambda_p) &= \mathscr{H}_1[g(r); r \to \lambda_p] \\ \hat{g}(\lambda_p) &= \mathscr{H}_0[g(r); r \to \lambda_p]. \end{aligned} \tag{4.15}$$

The theory of finite Hankel transforms with (4.7) and (4.14), yields

$$\mathscr{H}_1[\mathscr{B}_1(f^{(n)}); r \to \lambda_p] = -\lambda_p^2 \bar{f}^{(n)}(\lambda_p). \tag{4.16}$$

Also, for an arbitrary function $g(r)$ (see [3], p. 87),

$$\mathscr{H}_1\left[\frac{dg}{dr}; r \to \lambda_p\right] = -\lambda_p \hat{g}(\lambda_p). \tag{4.17}$$

Then from the theory of finite Hankel transforms and (4.9) we obtain,

$$\mathscr{H}_0[\mathscr{B}_0(u_z^{(n)}); r \to \lambda_p] = aK^{(n)} J_0(\lambda_p a) - \lambda_p^2 \hat{u}_z^{(n)}(\lambda_p) \tag{4.18}$$

$$\mathscr{H}_0[\mathscr{B}_0(\phi^{(n)}); r \to \lambda_p] = aG^{(n)} J_0(\lambda_p a) - \lambda_p^2 \hat{\phi}^{(n)}(\lambda_p) \tag{4.19}$$

where constants $K^{(n)}$ and $G^{(n)}$ are defined as follows.

$$\begin{aligned} K^{(n)} &= u_{z,r}^{(n)}(a), \qquad n = 0, \ldots, N \\ G^{(n)} &= \phi_{,r}^{(n)}(a), \qquad n = 1, \ldots, N. \end{aligned} \tag{4.20}$$

Use of (4.10) and (4.14) along with a recurrence formula for Bessel functions gives

$$\mathscr{H}_0\left[\frac{1}{r}\frac{d}{dr}(rf^{(n)}); r \to \lambda_p\right] = \lambda_p \bar{f}^{(n)}(\lambda_p), \tag{4.21}$$

and we recall (see [3], p. 88).

$$\mathscr{H}_1[r; r\to\lambda_p] = \begin{cases} -\dfrac{a^2}{\lambda_p} J_0(\lambda_p a), & \lambda_p \neq 0 \\ 0, & \lambda_p = 0 \end{cases}$$

$$\mathscr{H}_0[c; r\to\lambda_p] = \begin{cases} 0, & \lambda_p \neq 0 \\ c\dfrac{a^2}{2}, & \lambda_p = 0. \end{cases} \tag{4.22}$$

Next we carry out for $\lambda_p > 0$ the indicated finite Hankel transforms on (4.4) and obtain with use of (4.16)–(4.22) the following linear system of equations.

$$(1+\delta_{no})\left[\rho\omega^2 - c_{11}\lambda_p^2 - \left(\frac{n\pi}{2b}\right)^2 c_{44}\right]\bar{f}^{(n)}(\lambda_p) + \frac{\pi}{2b}(-\lambda_p)\sum_{m=0}^{N}\{D_{mn}\hat{u}_z^{(m)}(\lambda_p)\}$$
$$+\frac{n\pi}{2b}(e_{21}+e_{16})\lambda_p\hat{\phi}^{(n)}(\lambda_p) = \left[(1+\delta_{no})\rho\omega^2 - \left(\frac{n\pi}{2b}\right)^2 c_{44}\right]C^{(n)}\left[\frac{a^2}{\lambda_p}J_0(\lambda_p a)\right]$$
$$-\frac{1}{b}\bar{F}_r^{(n)}(\lambda_p) \quad \text{for} \quad n = 0, \ldots, N$$
$$-\left(\frac{\pi}{2b}\right)\sum_{m=0}^{N}\{D_{nm}\lambda_p\bar{f}^{(m)}(\lambda_p)\} + (1+\delta_{no})\left[\rho\omega^2 - c_{44}\lambda_p^2 - \left(\frac{n\pi}{2b}\right)^2 c_{22}\right]\hat{u}_z^{(n)}(\lambda_p)$$
$$+\sum_{m=0}^{N}\{R_{pmn}\hat{\phi}^{(m)}(\lambda_p)\} = -(1+\delta_{no})c_{44}aK^{(n)}J_0(\lambda_p a)$$
$$-e_{16}\sum_{m=1}^{N}\{B_{mn}aG^{(m)}J_0(\lambda_p a)\} - \frac{1}{b}\hat{F}_z^{(n)}(\lambda_p) \quad \text{for} \quad n = 0, \ldots, N$$
$$\left(\frac{n\pi}{2b}\right)(e_{21}+e_{16})\lambda_p\bar{f}^{(n)}(\lambda_p) + \sum_{m=0}^{N}\{R_{pnm}\hat{u}_z^{(m)}\} + \left[\epsilon_{11}\lambda_p^2 + \left(\frac{n\pi}{2b}\right)^2\epsilon_{22}\right]\hat{\phi}^{(n)}(\lambda_p)$$
$$= -e_{16}\sum_{m=0}^{N}\{B_{nm}aK^{(n)}J_0(\lambda_p a)\} + \epsilon_{11}aG^{(n)}J_0(\lambda_p a) \quad \text{for} \quad n = 1, \ldots, N \tag{4.23}$$

where we have defined

$$R_{pmn} = e_{16}(-\lambda_p^2)B_{mn} + \left(\frac{\pi}{2b}\right)^2 e_{22}B_{nm}mn.$$

For $\lambda_0 = 0$ the application of the first order finite Hankel transform to the first of (4.4) gives a trivial result. However, the application of zero order finite Hankel transform to the second and third of (4.4) yields at $\lambda_0 = 0$

$$\left[(1+\delta_{no})\rho\omega^2 - \left(\frac{n\pi}{2b}\right)^2 c_{22}\right]\hat{u}_z^{(n)}(0) + \left(\frac{\pi}{2b}\right)^2 e_{22}\sum_{m=0}^{N}\{B_{nm}mn\hat{\phi}^{(m)}(0)\}$$
$$= -(1+\delta_{no})c_{44}aK^{(n)} - \sum_{m=1}^{N}\{e_{16}B_{mn}aG^{(m)}\} + \left(\frac{\pi}{2b}\right)a^2\sum_{m=0}^{N}\{D_{nm}C^{(m)}\} - \frac{1}{b}\hat{F}_z^{(n)}(0)$$
$$+\frac{n\pi}{2b}B_{no}e_{22}\frac{B}{b}\left(\frac{1}{2}a^2\right) \quad \text{for} \quad n = 0, \ldots, N$$
$$\left(\frac{\pi}{2b}\right)^2 e_{22}\sum_{m=1}^{N}\{B_{mn}mn\hat{u}_z^{(m)}(0)\} + \left(\frac{n\pi}{2b}\right)^2\epsilon_{22}\hat{\phi}^{(n)}(0)$$
$$= -e_{16}\sum_{m=0}^{N}\{B_{nm}aK^{(m)}\} + \epsilon_{11}aG^{(n)} - \left(\frac{n\pi}{2b}\right)(e_{16}+e_{21})C^{(n)}a^2 \quad \text{for} \quad n = 1, 2, \ldots, N. \tag{4.24}$$

We can now solve $3N+2$ linear equations (4.23) for $3N+2$ values $\bar{f}^{(n)}(\lambda_p)$, $\hat{u}_z^{(n)}(\lambda_p)$, $\hat{\phi}^{(n)}(\lambda_p)$ for all $\lambda_p > 0$. Also $2N+1$ linear equations (4.24) can be solved for $2N+1$ values $\hat{u}_z^{(n)}(0)$ and $\hat{\phi}^{(n)}(0)$. Then the inversion formulas (4.11) and (4.12) can be applied to obtain the following expressions for the field variables.

$$f^{(n)}(r) = \frac{2}{a^2} \sum_{\lambda_p > 0} \left\{ \bar{f}^{(n)}(\lambda_p) \frac{J_1(\lambda_p r)}{[J_0(\lambda_p a)]^2} \right\}$$

$$u_z^{(n)}(r) = \frac{2}{a^2} \sum_{\lambda_p \geq 0} \left\{ \hat{u}_z^{(n)}(\lambda_p) \frac{J_0(\lambda_p r)}{[J_0(\lambda_p a)]^2} \right\}$$

$$\phi^{(n)}(r) = \frac{2}{a^2} \sum_{\lambda_p \geq 0} \left\{ \hat{\phi}^{(n)}(\lambda_p) \frac{J_0(\lambda_p r)}{[J_0(\lambda_p a)]^2} \right\}. \tag{4.25}$$

The solutions are in terms of transforms of forcing functions as well as the yet-unknown $3N+2$ constants $C^{(n)}$, $K^{(n)}$ and $G^{(n)}$.

From (4.13), (4.14) and the general form of the expansions in (4.25), it can be easily verified that the field variables $u_r^{(n)}$, $u_z^{(n)}$ and $\phi^{(n)}$ already satisfy the conditions of axisymmetry, i.e.

$$u_r^{(n)}(0) = 0; \qquad u_{z,r}^{(n)}(0) = 0; \qquad \phi_{,r}^{(n)}(0) = 0. \tag{4.26}$$

Therefore we have only the following edge boundary conditions to use in the evaluation of constants $C^{(n)}$, $K^{(n)}$ and $G^{(n)}$.

$$\begin{aligned} &T_{rr}^{(n)} = 0 \quad \text{for} \quad n = 0, \ldots, N \\ &T_{rz}^{(n)} = 0 \quad \text{for} \quad n = 0, \ldots, N \qquad \text{at} \quad r = a \\ &\bar{D}_r^{(n)} = 0 \quad \text{for} \quad n = 1, \ldots, N. \end{aligned} \tag{4.27}$$

Substitution of (4.13), (4.14) and (4.20) into the second and third of (4.3) yields with (4.27)

$$(1+\delta_{no}) c_{44} K^{(n)} + e_{16} \sum_{m=1}^{N} \{B_{mn} G^{(m)}\} + \frac{\pi}{2b} c_{44} \sum_{m=1}^{N} \{m B_{mn} a C^{(m)}\} = 0$$

$$\text{for} \quad n = 0, 1, \ldots, N$$

$$e_{16} \sum_{m=0}^{N} \{B_{nm} K^{(m)}\} - \epsilon_{11} G^{(n)} + \frac{n\pi}{2b} e_{16} a C^{(n)} = 0$$

$$\text{for} \quad n = 1, \ldots, N. \tag{4.28}$$

We rewrite the first of (4.3) as follows:

$$T_{rr}^{(n)} = (1+\delta_{no}) c_{11} \frac{1}{r} (r u_r^{(n)})_{,r} + (1+\delta_{no})(c_{11} - c_{13}) \frac{1}{r} u_r^{(n)}$$

$$+ \frac{\pi}{2b} c_{12} \sum_{m=1}^{N} \{m B_{mn} u_z^{(m)}\} - \frac{n\pi}{2b} e_{21} \phi^{(n)} + 2\delta_{no} e_{21} \frac{B}{b}. \tag{4.29}$$

By (4.13) we have

$$\frac{1}{r} (r u_r^{(n)})_{,r} = \frac{1}{r} (r f^{(n)})_{,r} + 2C^{(n)}. \tag{4.30}$$

Because of (4.21) and the inversion formula (4.12) the following expansion is valid in the closed interval $[0, a]$.

$$\frac{1}{r} (r f^{(n)})_{,r} = \frac{2}{a^2} \sum_{\lambda_p \geq 0} \lambda_p \bar{f}^{(n)}(\lambda_p) \frac{J_0(\lambda_p r)}{[J_0(\lambda_p a)]^2}. \tag{4.31}$$

Now we substitute (4.30), (4.31), (4.13), (4.14) and the second and third of (4.25) into (4.29) and obtain with the first of (4.27)

$$(1+\delta_{no})c_{11}\left(\frac{2}{a^2}\right)\sum_{\lambda_p\geq 0}\left\{\frac{\lambda_p\bar{f}^{(n)}(\lambda_p)}{J_0(\lambda_p a)}\right\}+\frac{\pi}{2b}c_{12}\sum_{m=1}^{N}\left\{mB_{mn}\left(\frac{2}{a^2}\right)\sum_{\lambda_p\geq 0}\left\{\frac{\hat{u}_z^{(m)}(\lambda_p)}{J_0(\lambda_p a)}\right\}\right\}$$
$$-\frac{n\pi}{2b}e_{21}\left(\frac{2}{a^2}\right)\sum_{\lambda_p\geq 0}\left\{\frac{\hat{\phi}^{(n)}(\lambda_p)}{J_0(\lambda_p a)}\right\}+(1+\delta_{no})(c_{11}+c_{13})C^{(n)}+2\delta_{no}e_{21}\frac{B}{b}=0$$
$$\text{for}\quad n=0,1,\ldots,N. \tag{4.32}$$

In (4.32), in addition to the explicit presence of $C^{(n)}$, we also have $K^{(n)}$ and $G^{(n)}$ involved through the terms of $\bar{f}^{(n)}$, $\hat{u}_z^{(n)}$ and $\hat{\phi}^{(n)}$. The equations (4.28) and (4.32) form the set of $3N+2$ linear equations which determines the set of $3N+2$ constants $C^{(n)}$, $K^{(n)}$ and $G^{(n)}$.

When the circular layer is the active element of a circuit, B becomes another unknown constant. The additional equation associated with it is derived by substituting the solution (4.25) for the two-dimensional field variables into the circuit equation (2.12) and carrying out the indicated integrations over the middle surface area of the layer.

5. THE TRANSIENT RESPONSE OF A CIRCULAR LAYER AFTER A SUDDEN RELEASE FROM AN INITIAL DEFORMATION

In this section we consider the problem of the transient response of the circular layer shown in Fig. 2. The motion is caused by an initial radially symmetric static surface load which is released at time, $t=0$.

We are primarily interested in the voltage that appears between the faces of the layer. Therefore, we need only study the extensional component of the motion. For this purpose, we use the first order approximate theory, which is the lowest order theory that incorporates the above-mentioned voltage difference in its extensional field equations.

The field equations governing the 2-D extensional displacement components, $u_r^{(0)}(r,t)$ and $u_z^{(1)}(r,t)$ of the first order theory are determined from (4.4) to be the following

$$\mathcal{R}_1(u_r^{(0)})+\frac{\pi}{4b}\frac{c_{12}}{c_{11}}B_{10}u_{z,r}^{(1)}-\frac{\rho}{c_{11}}\ddot{u}_r^{(0)}=0,$$
$$\mathcal{R}_0(u_z^{(1)})-\frac{\pi}{2b}\frac{c_{12}}{c_{44}}B_{10}\frac{1}{r}(ru_r^{(0)})_{,r}-\left(\frac{\pi}{2b}\right)^2\frac{c_{22}}{c_{44}}u_z^{(1)}$$
$$-\frac{\rho}{c_{44}}\ddot{u}_z^{(1)}=\frac{1}{b}\left(\frac{\pi}{2b}\right)\frac{e_{22}}{c_{44}}B_{10}B(t). \tag{5.1}$$

The extensional boundary conditions are those of vanishing stress components $T_{rr}^{(0)}$ and $T_{rz}^{(1)}$ (see eqn 4.3) at the cylindrical edge and the symmetry conditions at the center:

$$\left.\begin{aligned}&c_{11}u_{r,r}^{(0)}+c_{13}\frac{1}{r}u_r^{(0)}+\left(\frac{\pi}{4b}\right)c_{12}B_{10}u_z^{(1)}=-\frac{e_{21}}{b}B(t)\\&u_{z,r}^{(1)}=0,\end{aligned}\right\}\ \text{at}\quad r=a$$
$$u_r^{(0)}=0,\qquad u_{z,r}^{(1)}=0\quad\text{at}\quad r=0. \tag{5.2}$$

We also need initial conditions which we specify as

$$\left.\begin{aligned}&u_r^{(0)}=f_0(r)+C_0r,\quad u_z^{(1)}=g_0(r)\\&\dot{u}_r^{(0)}=0,\quad \dot{u}_z^{(1)}=0\end{aligned}\right\}\ \begin{aligned}&\text{at } t=0\\&\text{for } 0\leq r\leq a.\end{aligned} \tag{5.3}$$

In the initial condition for $u_r^{(0)}$ we have anticipated a decomposition similar to that in (4.13). The functions $f_o(r)$, $g_o(r)$ and the constant C_o are to be determined by the specified initial static load

from the solution of the problem of Section 4 for the first order extensional theory at frequency $\omega = 0$. The terms f_o, g_o and C_o correspond in the terminology of Section 4 to $u_r^{(o)}$, $u_z^{(1)}$ and $C^{(o)}$, respectively. For the present problem, however, we define variables $f(r, t)$, $C(t)$ and $g(r, t)$ by

$$u_r^{(o)}(r, t) = f(r, t) + rC(t); \qquad u_z^{(1)}(r, t) = g(r, t) \tag{5.4}$$

where

$$C(t) = a^{-1}u_r^{(o)}(a, t); \qquad f(a, t) = 0.$$

In terms of the new variables f, g, C, we have the following initial-boundary value problem.

$$\left.\begin{aligned}
&\mathscr{B}_1(f) + \frac{\pi}{4b}\frac{c_{12}}{c_{11}}B_{10}g_{,r} - \frac{\rho}{c_{11}}\ddot{f} = \frac{\rho}{c_{11}}\ddot{C}r,\\
&\mathscr{B}_o(g) - \frac{\pi}{2b}\frac{c_{12}}{c_{44}}B_{10}\frac{1}{r}(rf)_{,r} - \left(\frac{\pi}{2b}\right)^2\frac{c_{22}}{c_{44}}g\\
&- \frac{\rho}{c_{44}}\ddot{g} = \frac{1}{b}\left(\frac{\pi}{2b}\right)\frac{e_{22}}{c_{44}}B_{10}B(t) + \frac{\pi}{b}\frac{c_{12}}{c_{44}}B_{10}C,\\
&f_{,r} + \frac{\pi}{4b}\frac{c_{12}}{c_{11}}B_{10}g = -b^{-1}\frac{e_{21}}{c_{11}}B - \left(\frac{c_{11}+c_{13}}{c_{11}}\right)C,\\
&g_{,r} = 0
\end{aligned}\right\} \text{ at } r = a,\ t \geq 0$$

$$f = 0, \quad g_{,r} = 0; \quad \text{at} \quad r = 0, t \geq 0$$

$$f(r, 0) = f_o(r), \quad g(r, 0) = g_o(r)$$

$$C(0) = C_o, \quad \dot{f}(r, 0) + \dot{C}(0)r = 0, \quad \dot{g}(r, 0) = 0. \tag{5.5}$$

We solve this initial-boundary value system by successive applications of Laplace and Hankel transforms. Let the Laplace transform of an arbitrary function of time, $h(t)$ be denoted by

$$\tilde{h}(p) = \mathscr{L}[h(t)] = \int_o^\infty h(t)\,e^{-pt}\,dt. \tag{5.6}$$

Then we apply the Laplace transform to the field equations and the boundary conditions in (5.5). With use of the initial conditions this results in the following boundary-value problem for ordinary differential equations.

$$\mathscr{B}_1(\tilde{f}) + \frac{\pi}{4b}\frac{c_{12}}{c_{11}}B_{10}\tilde{g}_{,r} - \frac{\rho}{c_{11}}p^2\tilde{f} = -\frac{\rho}{c_{11}}pf_o(r) + \frac{\rho}{c_{11}}rp^2\tilde{C} - \frac{\rho}{c_{11}}rpC_o,$$

$$\mathscr{B}_o(\tilde{g}) - \frac{\pi}{2b}\frac{c_{12}}{c_{44}}B_{10}\frac{1}{r}(r\tilde{f})_{,r} - \left[\left(\frac{\pi}{2b}\right)^2\frac{c_{22}}{c_{44}} + \frac{\rho}{c_{44}}p^2\right]\tilde{g} = -\frac{\rho}{c_{44}}pg_o(r)$$

$$+ \frac{1}{b}\left(\frac{\pi}{2b}\right)\frac{e_{22}}{c_{44}}B_{10}\tilde{B} + \frac{\pi}{b}\frac{c_{12}}{c_{44}}B_{10}\tilde{C},$$

$$\left.\begin{aligned}
&\tilde{f}_{,r} + \frac{\pi}{4b}\frac{c_{12}}{c_{11}}B_{10}\tilde{g} = \left(\frac{-1}{b}\right)\frac{e_{21}}{c_{11}}\tilde{B} - \left(\frac{c_{11}+c_{13}}{c_{11}}\right)\tilde{C}\\
&\tilde{g}_{,r} = 0; \qquad \tilde{f} = 0
\end{aligned}\right\} \text{ at } r = a$$

$$\tilde{f} = 0, \quad \tilde{g}_{,r} = 0; \quad \text{at} \quad r = 0 \tag{5.7}$$

where the last of the boundary conditions at $r = a$ is obtained from the definition of f in (5.4).

As a first step toward the application of the Hankel transform we define a sequence of positive constants $\lambda_1, \lambda_2, \ldots$, as in (4.7). We then introduce the following notation for the doubly transformed variables

$$\bar{\bar{f}}(\lambda_n, p) = \mathcal{H}_1[\bar{f}(r, p); \quad r \to \lambda_n],$$
$$\hat{\bar{g}}(\lambda_n, p) = \mathcal{H}_0[\bar{g}(r, p); \quad r \to \lambda_n]. \tag{5.8}$$

We also need

$$\bar{f}_o(\lambda_n) = \mathcal{H}_1[f_o(r); \quad r \to \lambda_n], \qquad \hat{g}_o(\lambda_n) = \mathcal{H}_0[g_o(r); \quad r \to \lambda_n]. \tag{5.9}$$

Now we apply the first and zero order Hankel transforms, for $\lambda_n > 0$, to the first and second of (5.7), respectively. With the use of results from the theories of Hankel transforms and Bessel functions, the definition of λ_n, and the boundary conditions at $r = a$ in (5.7), we obtain the following linear system for determining $\bar{\bar{f}}(\lambda_n, p)$ and $\hat{\bar{g}}(\lambda_n, p)$.

$$(c_{11}\lambda_n^2 + \rho p^2)\bar{\bar{f}}(\lambda_n, p) + \frac{\pi}{4b} c_{12}B_{10}\lambda_n \hat{\bar{g}}(\lambda_n, p) = a^2\rho\lambda_n^{-1}J_0(\lambda_n a)[p^2\bar{C}(p) - pC(0)] + \rho p\bar{f}_o(\lambda_n)$$

$$\frac{\pi}{2b} c_{12}B_{10}\lambda_n \bar{\bar{f}}(\lambda_n, p) + \left[\lambda_n^2 c_{44} + \left(\frac{\pi}{2b}\right)^2 c_{22} + \rho p^2\right] \hat{\bar{g}}(\lambda_n, p) = \rho p \hat{g}_o(\lambda_n). \tag{5.10}$$

In the remaining analysis it is convenient to use dimensionless variables and parameters. We define these dimensionless (primed) quantities by

$$r' = r/a, \quad f' = f/a, \quad g' = g/b$$
$$t' = t \Big/ \frac{2b}{\pi}\sqrt{(\rho/c_{44})}, \quad c'_{ij} = c_{ij}/c_{44}, \quad e'_{ij} = e_{ij}/\sqrt{(c_{44}\epsilon_{22})}$$
$$V' = V/\sqrt{(b^2 c_{44}/\epsilon_{22})}, \quad Y' = Y/(\pi a^2 \epsilon_{22}/2b^2)\sqrt{(c_{44}/\rho)},$$
$$P' = P/\pi a^2 c_{44}, \tag{5.11}$$

where P represents a force (to be introduced later). Therefore,

$$\lambda'_n = \lambda_n a, \quad p' = p\tau, \quad \bar{f}' = \bar{f}/\tau a, \quad \bar{f}' = \bar{f}/a^3$$
$$\bar{g}' = \bar{g}/\tau b, \quad \bar{g}' = \bar{g}/a^2 b, \quad \tau = (2b/\pi)\sqrt{(\rho/c_{44})}. \tag{5.12}$$

We will omit the primes for economy of notation but with the understanding henceforth that all quantities are dimensionless. We also recall the value of B_{10} and introduce the parameter σ as

$$B_{10} = \sqrt{2}, \quad \sigma = (\pi a/2b)^2. \tag{5.13}$$

Using these results, we write in dimensionless form the solution of (5.10) as follows

$$\bar{\bar{f}}(\lambda_n, p) = \{\Theta_1(\lambda_n, p)\bar{C}(p) + \Theta_2(\lambda_n, p)[\bar{f}_o(\lambda_n) - C_o\lambda_n^{-1}J_0(\lambda_n)]$$
$$+ \Theta_3(\lambda_n, p)\hat{g}_o(\lambda_n)\}/\Psi(\lambda_n, p)$$
$$\hat{\bar{g}}(\lambda_n, p) = \{\Gamma_1(\lambda_n, p)\bar{C}(p) + \Gamma_2(\lambda_n, p)[\bar{f}_o(\lambda_n) - C_o\lambda_n^{-1}J_0(\lambda_n)]$$
$$+ \Gamma_3(\lambda_n, p)\hat{g}_o(\lambda_n)\}/\Psi(\lambda_n, p), \tag{5.14}$$

in which

$$\Psi(\lambda_n, p) = p^4\sigma^2 c_{11}^{-1} + p^2[(1 + c_{11}^{-1})\sigma\lambda_n^2 + \sigma^2 c_{22}c_{11}^{-1}] + \lambda_n^2 l(\lambda_n),$$
$$\Theta_1(\lambda_n, p) = \sigma p^2(\lambda_n^2 + \sigma c_{22} + \sigma p^2)J_0(\lambda_n)/c_{11}\lambda_n,$$
$$\Theta_2(\lambda_n, p) = p\sigma(\lambda_n^2 + \sigma c_{22} + \sigma p^2)/c_{11},$$
$$\Theta_3(\lambda_n, p) = -(\pi\sigma/2\sqrt{2})p\lambda_n c_{12}/c_{11},$$
$$\Gamma_1(\lambda_n, p) = -2\sqrt{2}\pi^{-1}\sigma^2 p^2 c_{12}J_0(\lambda_n)/c_{11},$$
$$\Gamma_2(\lambda_n, p) = -2\sqrt{2}\pi^{-1}\sigma^2 p\lambda_n c_{12}/c_{11}, \qquad \Gamma_3(\lambda_n, p) = \sigma p(\lambda_n^2 + \sigma p^2 c_{11}^{-1}), \tag{5.15}$$

where $l(\lambda_n)$ is defined by

$$l(\lambda_n) = \lambda_n^2 + \sigma c_{22} - \sigma c_{12}^2 c_{11}^{-1}. \tag{5.16}$$

Next we apply the appropriate Hankel transforms to the first two equations in (5.7) for $\lambda_n = \lambda_0$. The first equation yields nothing new, but the second one produces the result

$$(p^2 + c_{22})\hat{\bar{g}}(0, p) + \sqrt{2}\pi^{-1}e_{22}\tilde{B}(p) + 2\sqrt{2}\pi^{-1}c_{12}\tilde{C}(p) = p\hat{g}_o(0). \tag{5.17}$$

In order to satisfy the remaining boundary condition, which is the first in (5.7) at $r = a$, we must apply the inverse Hankel transforms to $\bar{f}(\lambda_n, p)$ and $\hat{\bar{g}}(\lambda_n, p)$ in (5.14) to obtain

$$\bar{f}(r, p) = 2\sum_{\lambda_n > 0} J_1(\lambda_n r)\bar{\bar{f}}(\lambda_n, p)/J_0^2(\lambda_n),$$
$$\bar{g}(r, p) = \hat{\bar{g}}(0, p) + 2\sum_{\lambda_n > 0} J_0(\lambda_n r)\hat{\bar{g}}(\lambda_n, p)/J_0^2(\lambda_n). \tag{5.18}$$

Then the substitution of (5.18) into the remaining boundary condition yields, with use of (5.14)

$$(\pi/\sqrt{2})c_{12}\hat{\bar{g}}(0, p) + e_{21}\tilde{B}(p) + (c_{11} + c_{13})\tilde{C}(p)$$
$$+ 2\sum_{\lambda_n > 0}\{[\lambda_n c_{11}\Theta_1 + (\pi/2\sqrt{2})c_{12}\Gamma_1]\tilde{C}(p)$$
$$+ [\lambda_n c_{11}\Theta_2 + (\pi/2\sqrt{2})c_{12}\Gamma_2][\bar{f}_n(\lambda_n) - C_o J_0(\lambda_n)\lambda_n^{-1}]$$
$$+ [\lambda_n c_{11}\Theta_3 + (\pi/2\sqrt{2})c_{12}\Gamma_3]\hat{g}_o(\lambda_n)\}/J_0(\lambda_n)\Psi = 0. \tag{5.19}$$

This result and (5.17) give two equations in the three variables $\hat{\bar{g}}(0, p)$, $\tilde{B}(p)$ and $\tilde{C}(p)$. A third equation is obtained from the circuit equation (2.12), which for the first order theory in axisymmetric dimensionless form becomes

$$-\dot{B}(t) + 2e_{21}\dot{C}(t) + \pi e_{22}\hat{\bar{g}}(0, t) = 2\pi^{-1}YB(t). \tag{5.20}$$

Application of the Laplace transform to this equation yields

$$-(p + 2\pi^{-1}Y)\tilde{B}(p) + 2pe_{21}\tilde{C}(p) + \pi e_{22}p\hat{\bar{g}}(0, p)$$
$$= 2e_{21}C_o + \pi e_{22}\hat{g}_o(0), \tag{5.21}$$

in which we have set

$$B(0) = 0, \tag{5.22}$$

representing steady-state closed circuit conditions before the initial static load is released.

Solving (5.17), (5.19) and (5.21) for $\bar{B}(p)$, $\bar{C}(p)$ and $\bar{\hat{g}}(0,p)$, we obtain for $\bar{B}(p)$ the expression

$$\bar{B}(p)=\frac{P_1^{(2)}(p)+2p^2\sum_{\lambda_n>0}P_2^{(4)}(\lambda_n,p)/\Psi(\lambda_n,p)}{P_3^{(3)}(p)-2\sigma p^2\sum_{\lambda_n>0}P_4^{(5)}(\lambda_n,p)/\Psi(\lambda_n,p)} \tag{5.23}$$

in which $\Psi(\lambda_n,p)$ is defined in (5.15) and $P_1^{(2)}(p)$, $P_2^{(4)}(\lambda_n,p)$, $P_3^{(3)}(p)$ and $P_4^{(5)}(\lambda_n,p)$ are second, fourth, third and fifth order polynomials in p, respectively. They are explicitly defined as follows:

$$\begin{aligned}
P_1^{(2)}(p)&=p^2e_{21}[(\pi/\sqrt{2})c_{12}\hat{g}_o(0)+(c_{11}+c_{13})C_o]\\
&\quad+[c_{22}(c_{11}+c_{13})-2c_{12}^2][e_{21}C_o+(\pi/2)e_{22}\hat{g}_o(0)],\\
P_2^{(4)}(\lambda_n,p)&=p^4\sigma^2e_{21}[\lambda_n\bar{f}_o(\lambda_n)+(\pi/2\sqrt{2})c_{12}c_{11}^{-1}\hat{g}_o(\lambda_n)]/J_0(\lambda_n)\\
&\quad+p^2\{[\sigma e_{21}l(\lambda_n)-\sigma^2(\sqrt{2}e_{22}c_{12}-c_{22}e_{21})]\lambda_n\bar{f}_o(\lambda_n)/J_0(\lambda_n)\\
&\quad+(\pi\sigma^2/2)c_{12}c_{11}^{-1}[(1/\sqrt{2})c_{22}e_{21}-c_{12}e_{22}]\hat{g}_o(\lambda_n)/J_0(\lambda_n)\\
&\quad+(\pi\sigma^2/2)e_{22}c_{22}\hat{g}_o(0)+\sigma^2\sqrt{2}c_{12}e_{22}C_o\}\\
&\quad+\sigma l(\lambda_n)[(c_{22}e_{21}-\sqrt{2}c_{11}e_{22})\lambda_n\bar{f}_o(\lambda_n)/J_0(\lambda_n)\\
&\quad+(\pi/2)c_{22}e_{22}\hat{g}_o(0)+(\sqrt{2})c_{12}e_{22}C_o],\\
P_3^{(3)}(p)&=p^3[-e_{21}^2-(c_{11}+c_{13})/2]+p^2[-Y\pi^{-1}(c_{11}+c_{13})]\\
&\quad+p[(1+\sqrt{2})c_{12}e_{21}e_{22}-c_{22}e_{12}^2-(c_{11}+c_{13})(c_{22}+\sqrt{2}e_{22}^2)/2]\\
&\quad+Y\pi^{-1}[2c_{12}^2-c_{22}(c_{11}+c_{13})],\\
P_4^{(5)}(\lambda_n,p)&=p^5\sigma/2+p^4\sigma Y\pi^{-1}+p^3[l(\lambda_n)/2+\sigma(c_{22}+\sqrt{2}e_{22}^2)/2]\\
&\quad+p^2Y\pi^{-1}[l(\lambda_n)+\sigma c_{22}]+pl(\lambda_n)(c_{22}+\sqrt{2}e_{22}^2)/2+Y\pi^{-1}c_{22}l(\lambda_n)
\end{aligned} \tag{5.24}$$

in which $l(\lambda_n)$ is defined in (5.16). The quantities $\bar{f}_o(\lambda_n)$, $\hat{g}_o(\lambda_n)$, C_o and $\hat{g}(0)$ appearing in $P_1^{(2)}(p)$ and $P_2^{(4)}(\lambda_n,p)$ are determined by the initial conditions given in (5.5).

If the infinite series in (5.23) are approximated by their first m terms, $\bar{B}(p)$ can be expressed as a quotient of two polynomials in p:

$$\bar{B}(p)=Q^{(2+4m)}(p)/R^{(3+4m)}(p). \tag{5.25}$$

Disregarding cases in which $R^{(3+4m)}(p)$ has repeated roots, the quotient in (5.25) can be expressed as a sum of partial fractions such as

$$\frac{A}{p+a},\qquad\frac{Ep+F}{p^2+2r_1p+(r_1^2+r_2^2)}, \tag{5.26}$$

where $p+a$, $p+r$ and $p+\bar{r}$ $(r=r_1+ir_2)$ represent real and complex conjugate factors of $R^{(3+4m)}(p)$. The corresponding inverse Laplace transforms are

$$Ae^{-at},\qquad Ee^{-r_1t}\cos(r_2t)+(-Er_1+F)r_2^{-1}e^{-r_1t}\sin(r_2t). \tag{5.27}$$

The electric potential difference between the two electroded surfaces, $2B(t)$, is therefore obtained by a summation of terms such as those in (5.27).

The series in (5.23) converge like $1/\lambda_n^2$ and therefore like $1/n^2$. This means that the number, m, of terms required for a suitable approximation may be too large for this inversion scheme to be practical. In this case a numerical inversion technique, such as one based on the Fast Fourier Transform, is likely to be preferable. This will be examined in the context of a particular example in the next section.

6. AN EXAMPLE

We now consider a specific example of the static initial mechanical loading on the piezoelectric layer. Let the radial component of the facial loads vanish and let the axial loads consist of a central concentrated force P, on one side with a balancing uniform peripheral load on the other. This loading configuration can be thought of as the limiting case of that given below as $r_o \to 0$.

$$F_r^{(0)} = 0; \quad F_z^{(1)} = p_o[1 - H(r - r_o) + H(r - r_1)], \tag{6.1}$$

where $F_r^{(0)}$ and $F_z^{(1)}$ are given in (4.6), H stands for the Heaviside function and

$$r_1 = (a^2 - r_0^2)^{1/2}; \quad p_o = P/\pi r_o^2. \tag{6.2}$$

From (4.15) we find

$$\bar{F}_r^{(0)}(\lambda_n) = 0 \quad \hat{F}_z^{(1)}(\lambda_0) = P/\pi$$
$$\hat{F}_z^{(1)}(\lambda_n) = (P/\pi\lambda_n)[r_o^{-1}J_1(\lambda_n r_o) - r_1 r_o^{-2}J_1(\lambda_n r_1)], \quad \lambda_n > 0. \tag{6.3}$$

In the limit $r_o \to 0$ this yields

$$\lim_{r_o \to 0} \hat{F}_z^{(1)}(\lambda_n) = (P/2\pi)[1 + J_0(\lambda_n a)], \quad \lambda_n > 0.$$

Using this and the first of (6.3) in the first order equations in (4.23) with $\omega = 0$, we obtain in dimensionless form

$$\lambda_n \bar{f}_o(\lambda_n) + (\pi/2\sqrt{2})c_{12}c_{11}^{-1}\hat{g}_o(\lambda_n) = 0,$$
$$2\sqrt{2}\sigma\pi^{-1}c_{12}\lambda_n \bar{f}_o(\lambda_n) + (\lambda_n^2 + \sigma c_{22})\hat{g}_o(\lambda_n) = 2\sigma P\pi^{-2}[1 + J_0(\lambda_n)], \quad \lambda_n > 0 \tag{6.5}$$

which has the solution

$$\bar{f}_o(\lambda_n) = -\sigma P c_{12}c_{11}^{-1}[1 + J_0(\lambda_n)]/\sqrt{2}\pi\lambda_n l(\lambda_n),$$
$$\hat{g}_o(\lambda_n) = 2\sigma P[1 + J_0(\lambda_n)]/\pi^2 l(\lambda_n), \quad \lambda_n > 0, \tag{6.6}$$

where $l(\lambda_n)$ is defined in (5.16). It still remains to determine C_o and $\hat{g}_o(0)$. Two equations for determining them are obtained from the first of (4.24) and (4.32). After elimination of $B(0)$ and also $K^{(1)}$ by the use of the second of (5.6) we obtain from the first of (4.24)

$$(\pi/2)c_{22}\hat{g}_o(0) + \sqrt{2}c_{12}C_o = 2\pi^{-1}P. \tag{6.7}$$

Use of (6.5) in (4.32) yields

$$(\pi/\sqrt{2})c_{12}\hat{g}_o(0) + (c_{11} + c_{13})C_o = 0. \tag{6.8}$$

These two equations determine $\hat{g}_o(0)$ and C_o as

$$\hat{g}_o(0) = 4\pi^{-2}P(c_{11} + c_{13})/[c_{22}(c_{11} + c_{13}) - 2c_{12}^2],$$
$$C_o = -2\sqrt{2}\pi^{-1}Pc_{12}/[c_{22}(c_{11} + c_{13}) - 2c_{12}^2]. \tag{6.9}$$

Equations (6.6) and (6.9) supply the $\bar{f}_o(\lambda_n)$, $g_o(\lambda_n)$, C_o and $\hat{g}_o(0)$ needed to completely determine $\tilde{B}(p)$ in (5.23) with the use of (5.24). Making the indicated substitutions we obtain

$$\tilde{B}(p) = \frac{Q_1^{(0)}(p) + 2p^2 \sum_{\lambda_n > 0} Q_2^{(2)}(\lambda_n, p)/\Psi(\lambda_n, p)}{Q_3^{(3)}(p) - 2\sigma p^2 \sum_{\lambda_n > 0} Q_4^{(5)}(\lambda_n, p)/\Psi(\lambda_n, p)} \tag{6.10}$$

in which $\Psi(\lambda_n, p)$ is defined in (5.15) and the polynomials $Q_k^{(m)}$ are defined as follows

$$\begin{aligned} Q_1^{(0)}(p) &= 2\pi^{-1} P[e_{22}(c_{11} + c_{13}) - \sqrt{2} c_{12} e_{21}], \\ Q_2^{(2)}(\lambda_n, p) &= \sigma^2 \pi^{-1} P\{2e_{22} - (c_{12} e_{21}/\sqrt{2} c_{11})[1 + J_0(\lambda_n)]/J_0(\lambda_n)\} p^2 \\ &\quad + \sigma \pi^{-1} P\{2e_{22} I(\lambda_n) - (\sigma c_{12}/\sqrt{2} c_{11}) \\ &\quad \times (c_{22} e_{21} - \sqrt{2} c_{12} e_{22})[1 + J_0(\lambda_n)]/J_0(\lambda_n)\} \\ Q_3^{(3)}(p) &= P_3^{(3)}(p), \quad Q_4^{(5)}(\lambda_n, p) = P_4^{(5)}(\lambda_n, p), \end{aligned} \tag{6.11}$$

where $P_3^{(3)}(p)$ and $P_4^{(5)}(\lambda_n, p)$ are given in (5.24).

The particular piezoelectric disk chosen for numerical computations is a Vernitron F-3 PZT-5 ceramic with the following physical parameters

$$\begin{gathered} a = 0.0125 \text{ m}, \quad b = 0.000625 \text{ m}, \quad \rho = 7.75 \times 10^3 \text{ kg/m}^3, \\ c_{44} = 2.11 \times 10^{10} \text{ N/m}^2, \quad \epsilon_{22} = 7.35 \times 10^{-9} \text{ C/Vm} \\ c_{11}/c_{44} = 5.73, \quad c_{22}/c_{44} = 5.26, \quad c_{13}/c_{44} = 3.57 \\ c_{12}/c_{44} = 3.56, \quad e_{22}/\sqrt{(\epsilon_{22} c_{44})} = 1.27, \quad e_{21}/\sqrt{(\epsilon_{22} c_{44})} = -0.434. \end{gathered}$$

The circuit to which the crystal is connected is assumed to have an input impedance of 50 Ω, so that

$$Y = 0.02\, \Omega^{-1}. \tag{6.13}$$

(i) *Approximate Laplace inversion using residue theory*

In Section 5 the function $\tilde{B}(p)$ was represented in (5.25) as a ratio of polynomials $Q^{(2+4m)}(p)$ and $R^{(3+4m)}(p)$, where m is the number of terms retained in the series in (5.23), or equivalently, in (6.10). We considered the cases $m = 1$, 2 and 3, which give simple poles of the approximate function $\tilde{B}(p)$ in the complex p-plane that yield dimensional frequencies according to (5.27) as listed in Table 1. We see that the frequencies that occur for $m = 1$ also occur for $m = 2$ and $m = 3$, and those that occur for $m = 2$ also occurs for $m = 3$ with only slight displacement. The new frequencies that appear as m increases are interlaced between the previous ones. The time histories corresponding to the $m = 1$, 2 and 3 term approximations, as obtained from (5.27), are shown in Fig. 3. Here we see that the convergence does not appear to be rapid. For this reason an alternate numerical inversion scheme was used.

(ii) *Approximate Laplace inversion using Fast Fourier Transform*

Consider the Laplace transform of a function $h(t)$ and its corresponding inversion

$$\tilde{h}(p) = \int_0^\infty h(t)\, e^{-pt}\, dt; \qquad h(t) = \frac{1}{2\pi i} \int_{c-i\infty}^{c+i\infty} \tilde{h}(p)\, e^{pt}\, dp, \tag{6.13}$$

where c locates the path of integration in the complex p-plane to the right of the poles of $\tilde{h}(p)$. In the application of interest here we can take $c = 0$. Next consider the Fourier transform and

Table 1

1 Term		2 Terms		3 Terms	
Laplace	FFT	Laplace	FFT	Laplace	FFT
0.093	0.0950	0.0878	0.0855	0.0855	0.0850
		0.2248	0.2300	0.2188	0.2200
				0.3465	0.3450
1.2654		1.2234	(1.1700)	1. 2086	(1.1900)
		1.5300	1.5300	1.5288	1.5300
				1.5550	1.5550
1.6689	(1.6300)	1.7005	(1.6660)	1.7139	(1.6950)

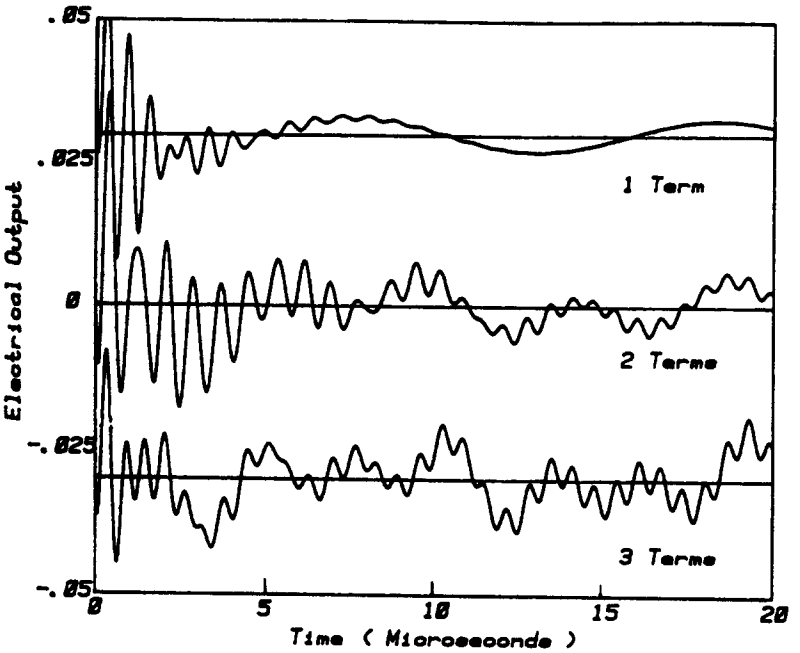

Fig. 3. Free-vibration electrical output of piezoelectric transducer element (Laplace inversion).

its inversion of a function $h(t)$ that vanishes for $t<0$,

$$\hat{h}(f)=\int_0^\infty h(t)\,e^{-i2\pi ft}\,dt; \qquad h(t)=\int_{-\infty}^{\infty}\hat{h}(f)\,e^{i2\pi ft}\,df. \tag{6.14}$$

When $c=0$ the transform pairs in (6.13) and (6.14) become identical through the substitution

$$p=i2\pi f. \tag{6.15}$$

Furthermore the Fourier transform pair as given in (6.14) is the form used as the basis for the Fast Fourier Transform (see Brigham[5]). From (6.13)–(6.15) it follows that

$$\tilde{h}(p)=\tilde{h}(i2\pi f)=\hat{h}(f). \tag{6.16}$$

Therefore the substitution of (6.15) into $\tilde{B}(p)$ of (6.10) produces $\hat{B}(f)$ which can be calculated for 2^N equally spaced points $\{f_k\}$. The result of this computation is a sequence of complex

numbers $\{\hat{B}(f_k)\}$ which must be properly arranged to insure that the inverse FFT will produce the correct real time history. We choose Δf and N such that the entire frequency spectrum is contained in the interval $0 \leq f \leq [(2^N/2)+1]\Delta f$. Then the real part of $\{\hat{B}(f_k)\}$ is reflected evenly about the mid-point $k = (2^N/2)+1$ while the imaginary part is reflected oddly. This insures periodicity in the frequency domain of period F, and corresponds to a sampling interval in the time domain of $\Delta t = 1/F$. Correspondingly, the period in the time domain is $T = 1/\Delta f$.

The technique just described was used to calculate $B(t)$ from (6.10) and (6.15). The series in (6.10) were terminated after m terms and it was found that suitable convergence was achieved for $m = 35$ but not for smaller values. Figure 4 shows the frequency spectrum for $m = 3$. The vertical scale on this graph is not absolute. The frequencies giving peaks in the spectra for $m = 1, 2$ and 3 are listed in Table 1, where they can be compared with those obtained from the Laplace inversion. If the poles in (5.25) lie close to the imaginary axis in the p-plane a sharp spike is produced in the frequency spectrum; otherwise a smoother maximum occurs as can be seen in Fig. 4 at 1.19 MHz. Peaks of this type are placed in parenthesis in Table 1. Also if the amplitude in (5.27) corresponding to a particular frequency is small, a high peak will not occur in the frequency spectrum.

Figures 5 and 6 show the frequency spectra for $m = 5$ and $m = 12$, respectively. We see that as m increases the low frequency part remains fixed and the higher frequency part fills in. Figures 7 and 8 show the frequency spectra for $m = 35$ and $m = 40$. These spectra are in complete agreement except for the highest frequency spike around 2.8 MHz. Evidently higher frequency spikes would continue to occur as m increases. Figures 9 and 10 show the time histories for $m = 3$ and 5 and $m = 35$ and 40. The differences between the $m = 3$ and 5 results are evident in Fig. 9, but the $m = 35$ and 40 results in Fig. 10 are nearly identical. When these graphs are superposed there are no important differences. These results were computed taking $N = 4096$ and $\Delta f = 5$ kHz. Only a portion of the first period was plotted in the time domain and in the frequency domain. The frequency period of the FFT is 20.48 MHz while the total time period is 200 μs. The corresponding time interval is about 0.05 μs. The failure of the time histories based on the FFT to satisfy the zero initial condition is due to the fact that the signal has not decayed to zero by the end of the time period, $T = 200$ μs. Therefore, the periodic time function has a discontinuity at $t = 0$ and the value produced there by the FFT is the average of the two limiting values. The differences in the time histories for $m = 3$ in Figs. 3 and 9 are not easily explained. Clearly the lower frequency parts are in agreement but the relative amplitude of the high frequency parts appears to be greater in Fig. 9 than in Fig. 3. Observe from Fig. 4

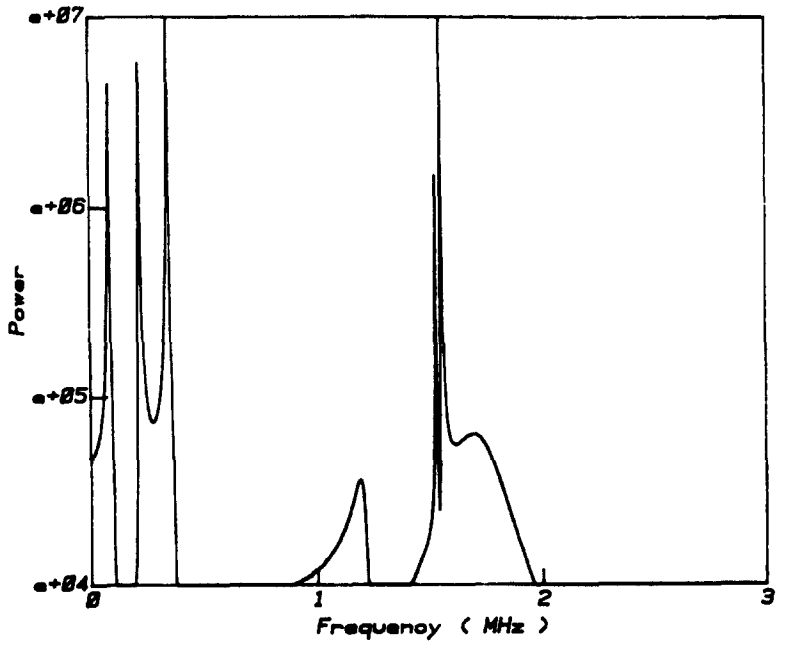

Fig. 4. Power spectrum (3 terms, FFT).

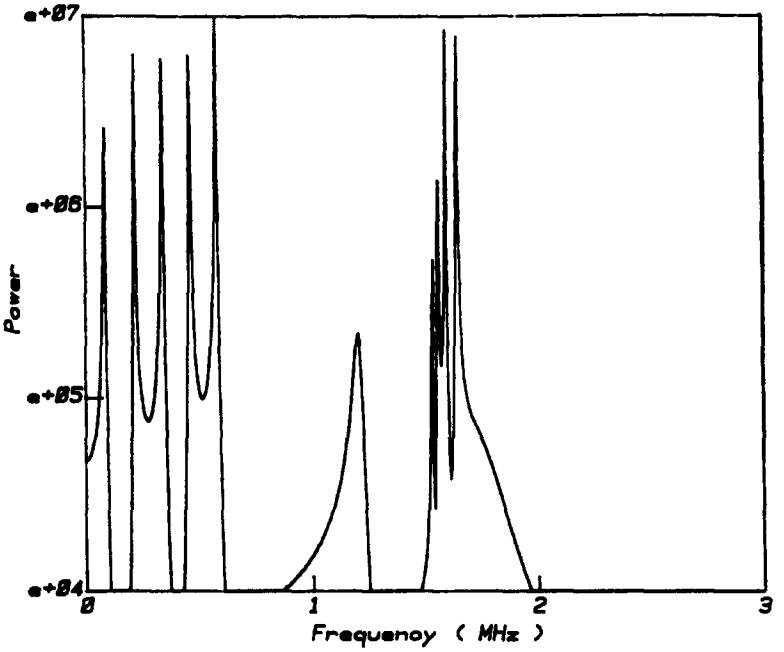

Fig. 5. Power spectrum (5 terms, FFT).

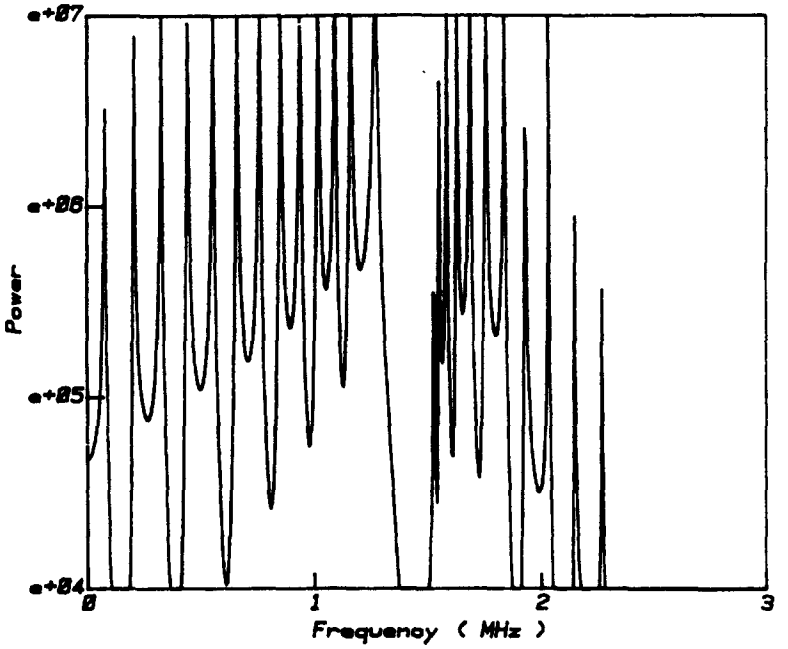

Fig. 6. Power spectrum (12 terms, FFT).

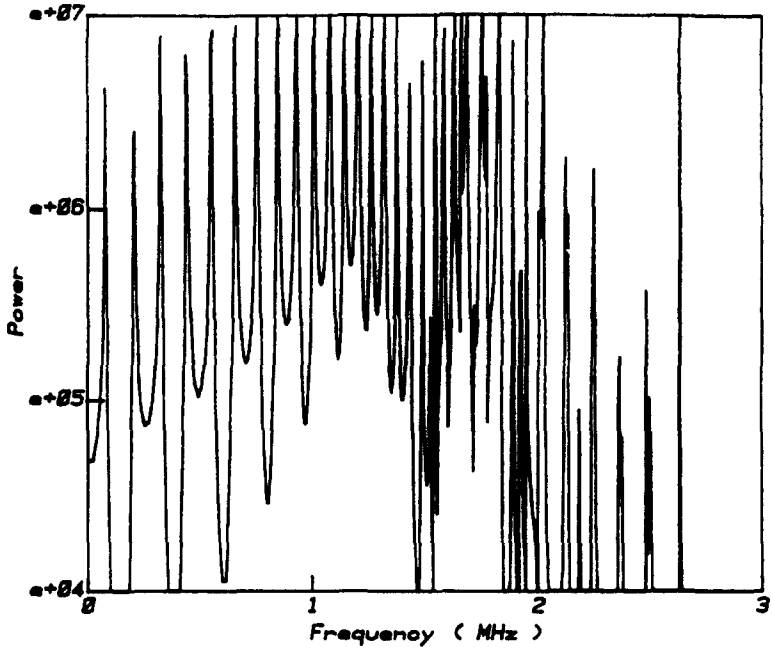

Fig. 7. Power spectrum (35 terms, FFT).

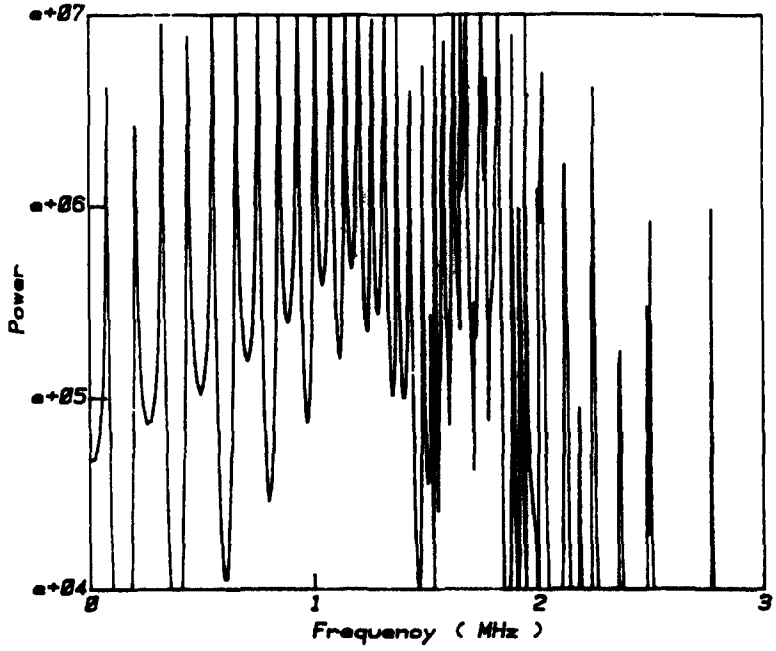

Fig. 8. Power spectrum (40 terms, FFT).

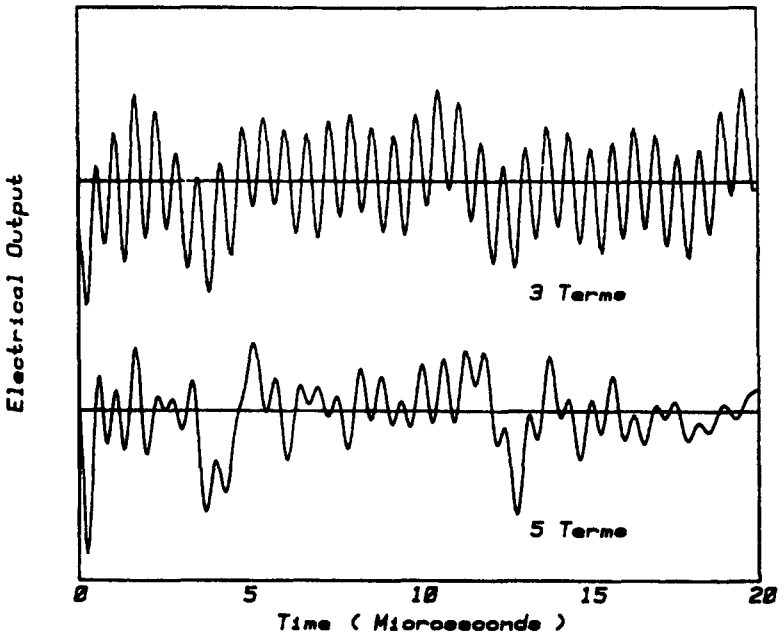

Fig. 9. Free-vibration electrical output of piezoelectric transducer element (FFT inversion).

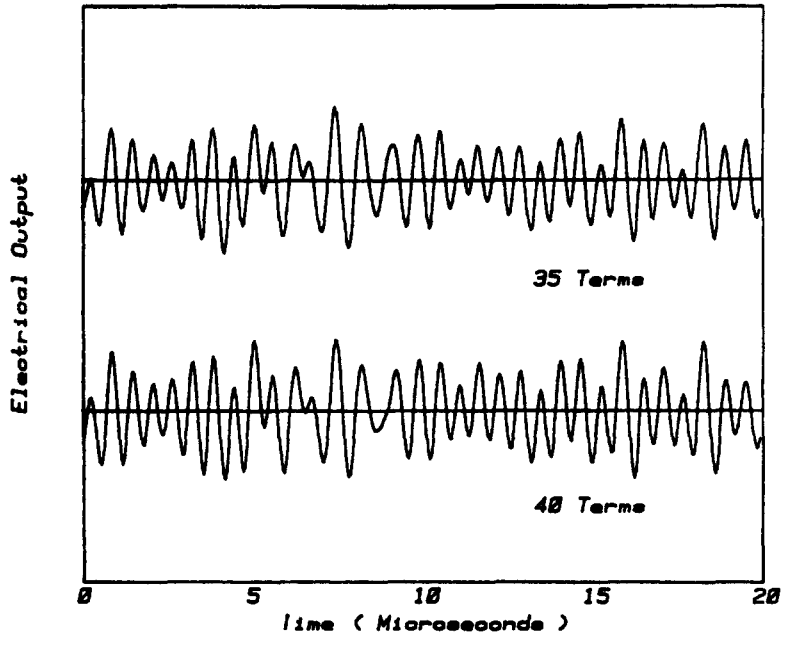

Fig. 10. Free-vibration electrical output of piezoelectric transducer element (FFT inversion).

that two high frequency spikes occur very close together. Table 1 indicates that one is at 1.5550 MHz, as obtained from both methods. The other is near 1.5300 MHz. Since the Δf used in the FFT method was 5 kHz this is the closest point to the value 1.5288 obtained by the Laplace method. The possible error in the location and hence the magnitude of this peak could cause it to combine with the neighboring peak in such a way as to account for the observed difference.

7. DISCUSSION AND CONCLUSIONS

The two dimensional approximate theory of Part I[1] for strongly coupled piezoelectric plates with electroded faces, which can accommodate arbitrary face loading and can be connected to an electric circuit, has been applied here to a PZT-5 crystal that is poled in its thickness direction. An important circuit equation was derived in Section 2. The steady time harmonic problems of plane strain and axisymmetry were solved in Sections 3 and 4, respectively. The transient axisymmetric problem was solved for arbitrary surface loads in Section 5, and this solution was applied to a particular loading case, that can be realized in the laboratory, in Section 6. There the output voltage as a function of time was calculated for a circular disk that is initially deformed by a central concentrated normal force and an oppositely directed ring load at its outer edge.

Two different techniques were used for inverting the Laplace transform of the output voltage. The first, which is practical when a small number of terms in the series in (6.10) are retained, uses residue theory, and it illustrates clearly the functional form of the components of the solution. In the second method the Fourier transform of the voltage is calculated, and this is inverted by use of a FFT computer algorithm. It was shown using this technique that 35–40 terms of the series in (6.10) must be retained to insure convergence. However, the higher terms of the series affect only the high frequency components of the output voltage. Most likely these high frequency components, in the 2 MHz range, would have relatively much less power in the corresponding experiment. It is expected that internal dissipation mechanisms, not accounted for in the theory, would reduce the power in these high frequencies. An experimental study of this and related problems will be the subject of a separate publication.

In comparing solutions of the type considered here with the corresponding experiments it may become necessary to use the second order approximate theory rather than the first order theory that we employed. However, for the crystal represented by (6.12) the dimensionless time, τ, in (5.12) is 2.41×10^{-7} sec. It follows from (4.4) of [1] that $\Omega = 1$ corresponds to 4.15×10^{6} H. Figure 4 of [1] indicates that the first order theory should be quite satisfactory up to this frequency.

Acknowledgements—This work was supported by the Solid Mechanics Program of the National Science Foundation under grant CME77-17150. The authors are indebted to D.K.-K. Miu for his assistance with the computations and graphics.

REFERENCES

1. N. Bugdayci and D. B. Bogy, A Two-dimensional Theory for Piezoelectric Layers Used in Electro-mechanical Transducers—I. Derivation. *Int. J. Solids Structures*, ms. 22.
2. O. Plaat, *Ordinary Differential Equations*. holden-Day, San Francisco (1971).
3. I. N. Sneddon, *Fourier Transforms*. McGraw-Hill, New York (1951).
4. G. N. Watson, *A Treatise on the Theory of Bessel Functions*. Cambridge University Press, Cambridge (1958).
5. E. O. Brigham, *The Fast Fourier Transform*. Prentice-Hall, New Jersey.